HHS Public Access

Author manuscript

J Physiol. Author manuscript; available in PMC 2020 August 01.

Published in final edited form as:

J Physiol. 2019 August ; 597(15): 3885–3903. doi:10.1113/JP277270.

Anti-inflammatory effects of oestrogen mediate the sexual dimorphic response to lipid-induced insulin resistance

João Paulo Camporez[1,2], **Kun Lyu**[1,3], **Emily L. Goldberg**[4,5], **Dongyan Zhang**[1], **Gary W. Cline**[1], **Michael J. Jurczak**[6], **Vishwa Deep Dixit**[4,5], **Kitt Falk Petersen**[1], **Gerald I. Shulman**[1,3,7]

[1]Department of Internal Medicine, Yale University School of Medicine, New Haven, CT 06520, USA

[2]Department of Physiology and Biophysics, Institute of Biomedical Sciences, University of Sao Paulo, Sao Paulo, Brazil 05508-000

[3]Cellular & Molecular Physiology, Yale University School of Medicine, New Haven, CT 06520, USA

[4]Comparative Medicine, Yale University School of Medicine, New Haven, CT 06520, USA

[5]Immunobiology, Yale University School of Medicine, New Haven, CT 06520, USA

[6]Department of Medicine, University of Pittsburgh, Pittsburgh, PA 15261, USA

[7]Howard Hughes Medical Institute, Yale University School of Medicine, New Haven, CT 06520, USA

Abstract

Oestrogen has been shown to play an important role in the regulation of metabolic homeostasis and insulin sensitivity in both human and rodent studies. Overall, females are protected against obesity-induced insulin resistance; yet, the mechanisms responsible for this protection are not well understood. Therefore, the aim of the present work was to evaluate the underlying mechanism(s) by which female mice are protected against obesity-induced insulin resistance compared with male mice. We studied male and female mice in age-matched or body weight-matched conditions. They were fed a high-fat diet (HFD) or regular chow for 4 weeks. We also studied HFD male mice treated with oestradiol or vehicle. Both HFD female and HFD male mice treated with oestradiol displayed increased whole-body insulin sensitivity, associated with reduction in ectopic hepatic and muscle lipid content compared to HFD male mice. Reductions in ectopic lipid content in these

Corresponding author J. P. Camporez: Department of Physiology and Biophysics, Institute of Biomedical Sciences, University of Sao Paulo, Sao Paulo, 05508-000, Brazil. camporez@usp.br.

Author contributions

J.P.C. designed research studies, conducted experiments, analysed data and wrote the manuscript. K.L. conducted experiments, analysed data, and contributed to discussion. E.G., M.J.J. and V.D.D. conducted experiments, analysed data, and contributed to discussion. K.F.P. contributed to discussion and wrote the manuscript. G.I.S. designed research studies, contributed to discussion and wrote the manuscript. J.P.C. is the guarantor of this work and, as such, has full access to all of the data in the study and takes responsibility for the integrity of the data and the accuracy of the data analysis. All authors have read and approved the final version of this manuscript and agree to be accountable for all aspects of the work in ensuring that questions related to the accuracy or integrity of any part of the work are appropriately investigated and resolved. All persons designated as authors qualify for authorship, and all those who qualify for authorship are listed.

Competing interests

The authors have declared that no conflict of interest exists.

mice were associated with increased insulin-stimulated suppression of white adipose tissue (WAT) lipolysis. Both HFD female and HFD male mice treated with oestradiol also displayed striking reductions in WAT inflammation, represented by reductions in plasma and adipose tissue tumour necrosis factor α and interleukin 6 concentrations. Taken together these data support the hypothesis that HFD female mice are protected from obesity-induced insulin resistance due to oestradiol-mediated reductions in WAT inflammation, leading to improved insulin-mediated suppression of WAT lipolysis and reduced ectopic lipid content in liver and skeletal muscle.

Introduction

Oestrogen has been shown to play an important role in the regulation of metabolic homeostasis and insulin sensitivity in both human and rodent studies. These beneficial effects of oestrogen on insulin action and glucose homeostasis are supported by studies showing that insulin sensitivity is greater in premenopausal women compared with age-matched men, and metabolism-related cardiovascular diseases and type 2 diabetes are less frequent in these same women (Nuutila *et al.* 1995; Donahue *et al.* 1997; Hoeg *et al.* 2009, 2011; Ribas *et al.* 2011; Mauvais-Jarvis *et al.* 2013). Also, it has been shown that lipid infusion-induced insulin resistance affects women less than men (Frias *et al.* 2001; Hoeg *et al.* 2011) and women in reproductive age display higher insulin sensitivity than men despite having higher intramuscular triacylglycerol (TAG) (Hoeg *et al.* 2009). Moreover, oestrogen replacement therapy in postmenopausal women reduces the incidence of type 2 diabetes (Margolis *et al.* 2004).

Experimental studies have also shown that oestrogen plays an important role in the regulation of metabolic homeostasis (Jones *et al.* 2000; Galbo *et al.* 2013; Camporez *et al.* 2013a). Increased body weight due to increased fat mass is observed in both ovariectomized mice (Camporez *et al.* 2013a) and ovariectomized rats (Camporez *et al.* 2011) and both female and male aromatase knockout mice, which are unable to synthesize oestrogen, have increased body weight, fat mass and adipocyte hyper-trophy compared with wild-type mice, demonstrating the impact of oestrogen deficiency on fat accumulation (Jones *et al.*2000). Some studies suggest that oestrogen's effects on metabolic homeostasis are mediated by oestrogen receptor α (ERα). Both male and female ERα knockout mice display increased weight gain and fat mass associated with impaired glucose tolerance (Heine *et al.* 2000), and *in vivo* activation of ERα enhances mitochondrial function and systemic metabolism in high fat-fed ovariectomized mice (Hamilton *et al.* 2016). At the same time, ERβ knockout mice do not display changes in body weight, fat mass or glucose tolerance (Foryst-Ludwig *et al.* 2008).

Moreover, it has been shown experimentally that female rodents are protected against lipid-induced insulin resistance compared with male rodents. Intralipid infusion in a rat study induced reduced insulin sensitivity in male rats while female rats were not affected (Hevener *et al.* 2002). Also, female rats are protected against high-fat diet (HFD)-induced glucose intolerance and insulin resistance associated with reduced inflammatory markers in adipose tissue compared with male rats (Estrany *et al.* 2011; Medrikova *et al.* 2012; Estrany *et al.*

2013) and it was observed that there was higher insulin sensitivity in adipocytes from female mice compared with male mice (Macotela *et al.* 2009).

Overall, females are protected against lipid-induced insulin resistance; yet, the mechanisms responsible for this protection are not well understood. Therefore, the aim of the present work was to evaluate the underlying mechanism(s) by which female mice are protected against obesity-induced insulin resistance compared with male mice. Here, based on our observation, we propose the cellular and physiological mechanisms associated with the sexual dimorphic nature of glucose and lipid metabolism that contribute to the differential susceptibility of female *vs.* male mice to lipid-induced insulin resistance in liver, skeletal muscle and white adipose tissue (WAT).

Methods

Ethical approval

All experimental procedures were approved by and conducted in accordance with the Institutional Animal Care and Use Committee guidelines of Yale University School of Medicine and followed the NIH *Guide for the Care and Use of Laboratory Animals*. Moreover, the authors understand, and the work conforms to, the principles and regulations of *The Journal of Physiology* (Grundy, 2015).

Animal care and protocol

All mice used in this study were C57BL6 acquired from The Jackson Laboratory (Bar Harbor, ME, USA). Experiments were performed in three different groups.(1) An age-matched study: male and female mice at 20 weeks of age were fed regular chow (RC) or HFD (60% fat (90% from lard and 10% from soybean oil), 20% carbohydrate, 20% protein; D12492, Research Diets, New Brunswick, NJ, USA) for 4 weeks. All the experiments were performed after the period of 4 weeks of diet. (2) Body weight-matched study: in order to perform a study with both male and female mice at similar body weight, we studied male mice at 8 week of age and female mice at 20 weeks of age. They were fed RC or HFD for 4 weeks before the experiments were performed. (3) Oestradiol (E2) treatment study: in order to study the effects of E2 treatment in male mice, 12-week-old male mice were fed HFD for 3 weeks, and then they were S.C. implanted with pellets releasing either placebo (vehicle) or E2 (0.1 mg for 60 days, i.e. 50 μg kg^{-1} day^{-1}; Innovative Research of America, Sarasota, FL, USA) and the experiments were performed 3 weeks after E2 pellet implantation. This dose of E2 was based on a previous study (Camporez *et al.* 2013a) and yielded physiological plasma concentration in male mice compared with age-matched female mice (plasma E2, pg ml^{-1}: vehicle, 6.4 ± 0.8; E2-treated male mice, 31.3 ± 2.5; female mice, 28.8 ± 2.0). During all procedures mice were in a constant room temperature environment, with 12:12 h light:dark cycle, with free access to water and food.

Fat and lean body mass were assessed by ^{1}H-magnetic resonance spectroscopy (Bruker BioSpin, Billerica, MA, USA). The Comprehensive Lab Animal Monitoring System (CLAMS; Columbus Instruments, Columbus, OH, USA) was used to evaluated O_2

consumption, CO_2 production, energy expenditure, activity and food consumption. Drinking was assessed by a computer system counting consumed water droplets.

Hyperinsulinaemic–euglycaemic clamps

The surgery for the hyperinsulinaemic–euglycaemic clamp was performed under isoflurane anaesthesia (5% for induction and 2.5% for maintenance). Carprofen was administrated S.C. (5 mg kg^{-1}) after the surgery. Hyperinsulinaemic–euglycaemic clamps were performed as previously described (Camporez *et al.* 2015). Mice had a jugular venous catheter implanted 7 days before hyperinsulinaemic–euglycaemic clamp. Whole-body glucose turnover was assessed by [3-^{3}H]glucose (HPLC purified; Perkin-Elmer Life Sciences, Waltham, MA, USA) infused at a rate of 0.05 μCi min^{-1} for 120 min into the jugular catheter after ~6 h fasting condition. Following the basal period, hyperinsulinaemic–euglycaemic clamps were performed in conscious mice for 140 min with a 3 min primed infusion of insulin (6.0 mU kg^{-1} min^{-1}) and [3-^{3}H]glucose (0.24 μCi min^{-1}), followed by a continuous (2.5 mU kg^{-1} min^{-1}) infusion of human insulin (Novolin; Novo Nordisk, Cambridge, MA, USA), and [3-^{3}H]glucose (0.1 μCi min^{-1}), and a variable infusion of 20% dextrose to maintain euglycaemia (100–120 mg dL^{-1}). To evaluate tissue-specific glucose uptake, a 10 μCi bolus of 2-deoxy-D-[1-^{14}C]glucose (Perkin-Elmer) was injected after 85 min to estimate the insulin-stimulated tissue glucose uptake. Plasma samples were obtained from the tip of the tail at 0, 25, 45, 65, 80, 90, 100, 110, 120, 130 and 140 min. The tail incision was made at least 2 h before the first blood sample was taken to allow for acclimatization, according to standard operating procedures. Basal and insulin-stimulated whole body glucose turnover rates (R_d) = ([3-^{3}H]glucose infusion (in dpm))/(plasma glucose specific activity (dpm mg $^{-1}$)) at the end of the basal period and during the final 40 min of the clamp, respectively. Endogenous glucose production = R_d − glucose infusion rate. Tissue 2-[^{14}C]deoxyglucose-6-phosphate content was measured following sample homogenizing, and the supernatant's 2-[^{14}C]deoxyglucose-6-phosphate was separated from 2-deoxyglucose with an ion exchange column. During both basal and clamped periods, mice were co-infused with sodium [U-^{13}C]palmitate (300 mg kg^{-1} min^{-1}) and [1,1,2,3,3-d5]glycerol (2.25 mmol kg^{-1} min^{-1}) and their plasma enrichments were measured by gas chromatography–mass spectrometry (GC-MS: HP6890–5975C, column: HP-101 25 m × 0.33 μm, CI ionization: isobutane). Briefly, [U-^{13}C]palmitate enrichment was determined as follows. Plasma lipids were extracted into ethyl ether, free fatty acids purified by silica thin layer chromatography (developed with hexane:ethyl ether:acetic acid, 60:13:0.65), derivatized as the fatty-acid methyl ester by reaction with BF_3–methanol, and analysed by GC-MS (m/z 271–287) (Wu *et al.* 2011). Briefly, [1,1,2,3,3-d5]glycerol enrichment was determined as follows. Plasma was deproteinized with equal volumes ZnSO4 (4 M), BaOH (4 M), dried under vacuum, and derivatized as the triacetate by reaction with acetic anhydride and pyridine, quenched with methanol and analysed by GC-MS (m/z 219–224) (Previs *et al.* 1999). Palmitate and glycerol turnover (stated here as whole-body lipolysis) were calculated as previously describes (Perry *et al.* 2015), using the formula below.

$$\text{Turnover} = \left(\frac{^{13}\text{C tracer enrichment}}{^{13}\text{C plasma enrichment}} - 1 \right) \times \text{Infusion rate}$$

At the end of the clamps, mice were anaesthetized with pentobarbital sodium injection (150 mg kg^{-1}) and all tissue samples taken were snap-frozen in liquid nitrogen and stored at −80°C for subsequent use. The skeletal muscle used was gastrocnemius + soleus and the white adipose tissue collected was the peri-gonadal for the male mice and peri-uterine for the female mice.

Tissue lipid measurement

The euthanasia for tissue harvesting was performed under isoflurane anaesthesia. Tissue triglycerides were extracted using the method of Folch *et al.* (1957) and measured using a Triglyceride-SL reagent (Seikisui Diagnostics, Lexington, MA, USA).

For ceramide extraction, approximately 50 mg of tissue was homogenized with 1 ml of methanol. Chloroform and a C17 internal standard were added. The sample was mixed well for 15 min. Water was then added to create an organic and aqueous phase. After centrifugation, the organic layer was collected, dried overnight in a vacuum oven, and reconstituted with chloroform. Lipid metabolite extract was subjected to liquid chromatography (LC)–tandem mass spectrometry (MS/MS) analysis. An atmospheric pressure chemical ionization source in positive mode was interfaced with a 6500 Qtrap tandem mass spectrometer (SCIEX, Framingham, MA, USA) in conjunction with a Shimadzu Prominence HPLC System (Shimadzu, Columbia, MD, USA). The following species were monitored using a multiple reaction monitoring (MRM) method: C16 520.6/264.2, C18 548.6/264.2, C20 576.8/264.2, C22 604.8/264.2, C24:1 631.0/264.2, C24 633.0/264.2 and IS C17 534.6/264.2. Total ceramide content was expressed as the sum of individual species.

For diacylglycerol (DAG), approximately 50 mg of tissue was homogenized in ice-cold $CHCl_3$–methanol (2:1 v/v) containing 0.01% butylated hydroxytoluene and the internal standards 1,2-dinonadecanoin and 1,2,3-triheptadecanoate. Water and chloroform were added to create an organic and aqueous phase. After centrifugation, the organic layer was collected, dried under nitrogen flow, and reconstituted with hexane–methylene chloride–ether (89/10/1 v/v/v). Diacylglycerol was separated from TAG with preconditioned diol columns (Waters Sep Pak Cartridge WAT020845; Waters, Milford, MA, USA) and eluted with hexane–ethyl acetate (85/15 v/v) under a low negative pressure. Lipid metabolite extracts were subjected to LC-MS/MS analysis. An Application Program Interface (API) source was interfaced with an API 6500 QTRAP tandem mass spectrometer (SCIEX) in conjunction with a Shimadzu Prominence HPLC System (Shimadzu). The following species were monitored using a MRM method: C16:0–16:0 551.6/239.3, C16:0–18:0 579.7/239.3, C16:0–18:1 577.6/239.3, C16:0–18:2 575.7/236.2, C18:0–18:0 607.7/267.3, C18:0–18:1 605.7/267.3, C18:0–18:2 603.7/267.3, C18:1–18:1 603.7/265.3, C18:1–18:2 601.7/265.3, C16:0–20:4 599.7/239.3, C18:0–20:4 627.7/267.3, C20:4–20:5 645.7/287.3, C17:0–17:0 579.7/253.3, C19:0–19:0 635.8/281.4. Total diacylglycerol content was expressed as the sum of individual species. To minimize any potential confounding effects of matrix effects on our LC-MS/MS analyses, all comparisons were made on relative differences between DAG/ceramide content in skeletal muscle of male *vs.* female mice or control *vs.* E2-treated mice analysed in the same LC-MS/MS run and relative differences between DAG/ceramide

content in liver tissue from male *vs.* female mice or control *vs.* E2-treated mice analysed in the same LC-MS/MS run.

All lipid measurements were made from tissues harvested from 6 h fasted mice.

Adipose immune profiling

Visceral adipose tissue was digested with collagenase I (1 mg ml^{-1} in Hanks' balanced salt solution) to separate the stromal vascular fraction (SVF). SVF was stained with live/dead viability dye (Thermo Fisher Scientific, Waltham, MA, USA), CD45, CD3, B220, CD11b, F4/80, CD11c and CD206 (from eBioscience (San Diego, CA, USA) and BioLegend (San Diego, CA, USA)) to gate T cells, B cells and macrophages. Data was acquired on an LSR II (BD Biosciences, San Jose, CA, US) and analysed in FlowJo (Treestar, Ashland, OR, USA). Samples were de-identified with regard to treatment (control *vs.* E2) for processing and analysis.

Immuno-blotting analysis

Tissues were homogenized in RIPA lysis buffer supplemented with protease inhibitor cocktail (Roche, New York, NY, USA) for protein isolation. Proteins from homogenized liver or skeletal muscle (60 μg of protein extracts) were electrophoretically separated by 4–12% SDS-PAGE (Thermo Fisher Scientific) and then transferred to polyvinylidene difluoride membranes (Millipore, Billerica, MA, USA) using a semidry transfer cell (Bio-Rad Laboratories, Hercules, CA, USA) for 120 min. After blockade of non-specific sites with 5% non-fat dry milk TBST (10 mM Tris, 100 mM NaCl, and 0.1% Tween 20) solution, membranes were incubated overnight at 4°C with the following primary antibodies: total Akt, total insulin receptor kinase (IRK), tyrosine pY1162 IRK (Santa Cruz Biotechnology, Inc., Dallas, TX, USA), Akt2 phosphorylation Ser^{474} (Cell Signaling Technology, Danvers, MA, USA), protein kinase C (PKC) ε (BD Transduction Laboratories, Lexington, KY, USA) and PKCθ (BD Transduction Laboratories). After washing with TBST, membranes were incubated with *horse-radish* peroxidase-conjugated anti-rabbit or anti-mouse secondary antibody. Membranes were thoroughly washed, and immune complexes were detected using an enhanced luminol chemiluminescence system (ECL; Thermo Fisher Scientific) and subjected to photographic films. Signals on the immuno-blot were quantified by optical densitometry (Scion Image software, Bethesda, MD, USA).

Plasma analyses

Plasma TAG concentrations were measured using a Triglyceride-SL reagent (Seikisui Diagnostics). Plasma fatty acids were determined with the NEFA C kit (Wako Pure Chemical Industries, Richmond, VA, USA). Plasma insulin concentrations were measured by RIA (Millipore). Plasma cytokines were measured using a mouse V-PLEX Proinflammatory Panel 1 (Meso Scale Discovery, Rockville, MD, USA) and adipose tissue cytokines were measured using a mouse inflammatory cytokine multi-analyte ELISArray kit (Qiagen, Germantown, MD, USA – product no. 336161, cat. no. MEM-004A).

Macrophages cell culture

J774 cells (ATCC® TIB-67™, acquired from ATCC, Manassas, VA, USA) were grown in RPMI-1640 medium without phenol red containing 10% fetal bovine serum (charcoal stripped – Thermo Fisher Scientific). This medium was supplemented with glutamine (2 mM), HEPES (20 mM), streptomycin (10,000 μg ml^{-1}), penicillin (10,000 UI ml^{-1}), and sodium bicarbonate (24 mM). Cells were grown in 75 ml flasks containing (0.5–1) × 10^6 cells ml^{-1}. The cells were kept in a humidified atmosphere containing 5% CO_2 at 37°C. The cells were diluted to 2.5 × 10^5 ml^{-1} in 24-well plate. On the following day, when the number of cells reached 5 × 10^5 ml^{-1}, they were treated with 100 μM of palmitate, or oestradiol (10 nM), or a specific ERα inhibitor (methyl-piperidino-pyrazole; MPP; 50 μM) for 24 h.

Statistical analysis

All data are expressed as means ± SEM. Results were assessed using two-tailed unpaired Student's *t* test or two-way ANOVA (Prism 5, GraphPad Software Inc., La Jolla, CA, USA). A *P* value less than 0.05 was considered significant.

Results

Age-matched mouse studies

First, we evaluated whole-body metabolism in age-matched mice (~20 weeks old). Male mice weighed more than female mice both after regular chow (RC) and after 4 weeks on a HFD (Table 1). Interestingly, the female mice fed RC had a higher percentage of whole-body fat as compared to male mice (Table 1), but there was no difference in percentage body fat in HFD-fed mice (Table 1). Fasting plasma insulin concentrations in HFD-fed mice were lower in female mice (Table 1) compared with male mice, suggesting greater whole-body insulin sensitivity. We also used a Comprehensive Lab Animal Monitoring System for simultaneous measurements of several metabolic parameters in RC-fed mice and found no difference between the groups in energy expenditure, respiratory exchange ratio (RER), caloric intake or water consumption (Table 1). Interestingly, female mice displayed a slightly higher ambulatory activity (Table 1). Next, in order to evaluate whole-body insulin sensitivity, hyperinsulinaemic–euglycaemic clamps were performed in age-matched female and male mice after RC and HFD feeding. There was no difference in insulin sensitivity between male and female mice fed RC (Fig. 1*A* and *B*), while HFD-fed male mice required a reduced glucose infusion rate (GIR) compared with RC-fed mice to maintain euglycaemia during the hyperinsulinaemic–euglycaemic clamp (Fig. 1*A* and *B*), demonstrating increased whole-body insulin resistance. However, HFD-fed female mice were protected against obesity-induced insulin resistance and displayed no reduction in GIR compared with RC female or HFD male mice (Fig. 1*A* and *B*). This protection against lipid-induced insulin resistance was accounted for by both peripheral and hepatic insulin action. Female mice fed HFD displayed higher whole-body insulin-stimulated peripheral glucose metabolism (Fig. 1*C*) compared with male mice, along with greater muscle and WAT glucose uptake (Fig. 1*D*). Also, female mice fed HFD presented higher insulin-stimulated suppression of endogenous glucose production compared with HFD-fed male mice (Fig. 1*E* and *F*). Lastly, improvements in hepatic and muscle insulin sensitivity in HFD-fed female mice were associated with greater suppression of plasma non-esterified fatty acid levels by insulin

(NEFA) (Fig. 1*G* and *H*), suggesting higher WAT insulin sensitivity and reduced WAT lipolysis in HFD-fed female compared with HFD-fed male mice.

Since previous studies have shown a strong causal relationship between ectopic lipid accumulation and hepatic and muscle insulin resistance (Cantley *et al.* 2013; Camporez *et al.* 2015; Samuel & Shulman, 2016), we measured ectopic lipid content as well as activation of PKCε and PKCθ, in liver and muscle respectively, in RC and HFD male and female mice. There was no difference in hepatic TAG (Fig. 2*A*) or diacylglycerol (DAG) content (Fig. 2*B*) between RC-fed male and female mice. However, HFD-fed female mice displayed lower hepatic TAG (Fig. 2*A*) and DAG content (Fig. 2*B*) compared with HFD-fed male mice, without any difference in hepatic ceramide content between any group (Fig. 2*C*). Lesser hepatic TAG and DAG content were associated with smaller hepatic PKCε activation in HFD-fed female mice compared with HFD-fed male mice (Fig. 2*D*). Moreover, HFD-fed female mice displayed lower muscle TAG (Fig. 2*E*) and DAG content (Fig. 2*F*) compared with HFD-fed male mice, again without any difference in muscle ceramide content (Fig. 2*G*). These results were associated with less muscle PKCθ activation in HFD-fed female compared with male mice (Fig. 2*H*).

Body weight-matched studies

Differences in body weight between study groups can confound the interpretation of hyperinsulinaemic–euglycaemic clamp studies. In order to avoid the differences in body weight between male and female mice during the evaluation of insulin sensitivity, we studied body weight-matched mice by varying age at the time of study. There was no difference in body weight between groups (8-week-old male *vs.* 20-week-old female) during either RC or HFD feeding (Table 2), but RC-fed female mice displayed a higher percentage body fat compared with RC-fed males. In contrast, there was no difference in percentage body fat between HFD-fed female and male mice (Table 2). Fasting plasma insulin concentrations were lower in HFD female mice compared with male mice (Table 2), suggesting improved whole-body insulin sensitivity. Also, there was no difference between groups in energy expenditure, RER, caloric intake, activity or water consumption (Table 2). Consistent with the results during age-matched studies where differences in body weight were present (Fig. 1), body weight-matched female mice fed HFD were protected against lipid-induced whole-body insulin resistance compared with male mice (Fig. 3*A* and *B*). This protection against insulin resistance in female mice was accounted for by greater insulin-stimulated muscle and WAT glucose disposal in HFD-fed mice (Fig. 3*C* and *D*), and larger hepatic insulin sensitivity (Fig. 3*E* and *F*). This improvement in hepatic insulin sensitivity and muscle glucose disposal in HFD-fed female mice was associated with higher insulin-stimulated insulin receptor kinase (IRK) tyrosine^{1162} phosphorylation and Akt2 phosphorylation in liver and Akt2 phosphorylation in muscle (Fig. 3*G*–*I*). The larger whole-body insulin sensitivity in HFD-fed female mice was associated with improved insulin-stimulated suppression of WAT lipolysis compared with male mice, determined as the absolute reduction in plasma NEFA concentration, as well as the change in the rate of glycerol and palmitate turnover in response to insulin (Fig. 3*J*–*L*).

To investigate whether differences in ectopic lipid accumulation were associated with the protection against lipid-induced insulin resistance in body weight-matched male and female mice, we measured hepatic and muscle lipid content after HFD feeding. Female mice displayed lower hepatic TAG (Fig. 4*A*) and DAG content (Fig. 4*B*), but no differences in ceramide levels (Fig. 4*C*). Smaller TAG and DAG content occurred in parallel with lower hepatic PKCε activation in female compared with male mice (Fig. 4*D*). Consistent with the less hepatic lipid content, female mice also displayed lower muscle TAG (Fig. 4*E*) and DAG content (Fig. 4*F*), without differences in muscle ceramide content (Fig. 4*G*). Similarly, lesser muscle TAG and DAG content were associated with lower muscle PKCθ activation in HFD-fed female compared with male mice (Fig. 4*H*).

Oestradiol-treated male mice studies

Previous studies have shown that oestradiol (E2) administration plays a pivotal role in the protection against obesity and insulin resistance in female mice (Jones *et al.* 2000; Galbo *et al.* 2013). Therefore, we next examined whether E2 treated HFD-fed male mice would be protected against lipid-induced insulin resistance. Interestingly, E2-treated male mice displayed reduced percentage body fat compared with vehicle-treated controls after HFD feeding (Table 3). Also, E2-treated mice manifested reduced fasting plasma insulin concentrations (Table 3), suggesting improved whole-body insulin sensitivity. E2 treatment also increased energy expenditure, caloric intake and drinking (Table 3), with no changes in activity (Table 3). Next, whole-body insulin action was evaluated by a hyperinsulinaemic–euglycaemic clamp combined with stable and radio-labelled tracers to assess insulin action in liver, muscle and WAT. Male mice treated with E2 required increased GIR to maintain euglycaemia, an indication of improved whole-body insulin sensitivity compared with vehicle-treated mice (Fig. 5*A*). The increased whole-body insulin sensitivity was accounted for by improved insulin-stimulated peripheral glucose metabolism (Fig. 5*B*), which in turn could be attributed to increased insulin-stimulated skeletal muscle and WAT glucose uptake (Fig. 5*C*), as well as improved hepatic insulin sensitivity (Fig. 5*D* and *E*). This improvement in hepatic insulin sensitivity and muscle glucose disposal in E2-treated mice was associated with increased insulin-stimulated IRK tyrosine^{1162} phosphorylation and Akt2 phosphorylation in liver and Akt2 phosphorylation in muscle (Fig. 5*F*–*H*). The protection against obesity-induced liver and skeletal muscle insulin resistance in E2-treated mice was also associated with improved insulin-stimulated suppression of WAT lipolysis (Fig. 5*I*–*L*).

Given the reduction in ectopic lipid accumulation in female mice and their protection against lipid-induced insulin resistance, we next evaluated ectopic lipid content in liver and skeletal muscle and novel PKC activation in HFD-fed vehicle and E2-treated male mice. Hepatic TAG (Fig. 6*A*) and DAG (Fig. 6*B*) were reduced in E2-treated compared with vehicle-treated mice, without differences in hepatic ceramide content (Fig. 6*C*). E2-treated mice also displayed reduced hepatic PKCε activation (Fig. 6*D*). Consistent with the reduction in hepatic lipid content, E2-treated mice displayed reduced muscle TAG (Fig. 6*E*) and DAG (Fig. 6*F*) content, without differences between groups in muscle ceramide content (Fig. 6*G*). Accordingly, muscle PKCθ activation was reduced in E2-treated mice (Fig. 6*H*).

Inflammation profiling evaluation

The WAT inflammation has been implicated in the pathogenesis of HFD-induced insulin resistance (Hotamisligil, 2006; Perry *et al.* 2015). In particular, the inability of insulin to suppress WAT lipolysis would increase the delivery of fatty acids to other tissues, causing insulin resistance (Perry *et al.* 2015). In order to evaluate whether WAT inflammation plays a role in the sexual dimorphism in lipid-induced insulin resistance, we examined plasma and WAT cytokine concentrations in HFD-fed male *vs.* female mice (body weight-matched mice), and HFD-fed vehicle *vs.* E2-treated male mice. There was no difference in plasma interleukin (IL)-1β levels between HFD-fed male and female mice (Fig. 7*A*), but female mice displayed significantly reduced plasma IL-6 levels (Fig. 7*A*), plasma interferon-γ (IFN-γ) (Fig. 7*A*), and plasma tumour necrosis factor α (TNF-α) compared with male mice (Fig. 7*A*). Consistent with the plasma cytokine levels, female mice displayed no difference in WAT IL-1β levels (Fig. 7*B*), and reduced WAT IL-6 (Fig. 7*B*), IFN-γ (Fig. 7*B*) and TNF-α levels (Fig. 7*B*). We next examined whether HFD-fed, E2-treated male mice would also display reduced inflammation compared with HFD-fed, vehicle-treated male mice. Plasma IL-1β, IL-6 and TNF-α (Fig. 7*C*) were reduced in E2-treated mice compared with vehicle-treated mice, without any difference in plasma IFN-γ (Fig. 7*C*). Consistent with plasma levels, E2-treated mice displayed reduced WAT IL-1β, IL-6 and TNF-α concentrations (Fig. 7*D*), without any difference in WAT IFN-γ (Fig. 7*D*). Also, in visceral adipose tissue, E2 treatment reduced the accumulation and absolute number of macrophages (Fig. 7*E–G*), which are well known to promote inflammation and metabolic dysfunction.

In order to evaluate whether E2 displays direct effects on macrophages, we performed a macrophage cell line culture, which has been shown to respond to palmitate, releasing cytokines (de Lima-Salgado *et al.* 2011). Therefore, these cells were treated with palmitic acid (for 24 h) in order to mimic the *in vivo* HFD-fed mice and induce inflammatory cytokine secretion. Palmitate treatment induced a dramatic increase in TNF-α and IL-6 concentration in the supernatant (Fig. 8). Interesting, E2 treatment protected against palmitate-induced increase in TNF-α and IL-6 concentration in the supernatant, reaching almost the vehicle-treated cells' levels (Fig. 8). The cells were also concomitantly treated with a pharmacological inhibitor of ERα. The inhibition of ERα prevented the protective effect of E2 against palmitate-induced inflammatory cytokine release (Fig. 8).

Discussion

Since most experimental and clinical research has not considered how sex differences might impact the experimental outcomes, it has been postulated that there is a need to incorporate the different sexes in experimental and clinical research in order to understand the mechanism by which metabolic processes differ by sex (Morselli *et al.* 2016). As a result, this gap in scientific knowledge has been recently recognized by the National Institutes of Health (NIH), which now mandates that NIH-supported studies be conducted in both sexes.

Epidemiological, clinical and molecular studies have suggested that oestrogen plays a critical role in metabolic homeostasis by regulating lipid and glucose metabolism (Barros & Gustafsson, 2011), and the loss of oestrogen may have profound effects on glucose homeostasis and insulin sensitivity in both post-menopausal women (Lovejoy *et al.* 2008)

and rodents (Jones *et al.* 2000; Rogers *et al.* 2009). In the present study, we found that endogenous oestrogen is important to protect against HFD-induced whole-body insulin resistance compared with male mice, and E2 treatment in male mice also protected against obesity-induced insulin resistance. Also, we showed that oestrogen plays an important role in modulating WAT inflammation and ectopic lipid accumulation in liver and skeletal muscle. These effects may be attributed in part to ERα as shown by the lack of E2-mediated protection *in vitro* on macrophages after a pharmacological ERα inhibition. These data are consistent with prior studies that implicated reduced signalling via ERα on macrophages as contributor towards increased insulin resistance and inflammation (Ribas *et al.* 2011). Although E2 did not alter M1-like or M2-like phenotypes (CD11c or CD206 expression, respectively – data not shown), this is not terribly surprising given that adipose tissue macrophages have a diverse phenotype and do not discretely fit into an M1/M2 paradigm (Camell *et al.* 2017). Other studies have also shown that female rodents are protected against HFD-induced insulin resistance associated with reduced adipose tissue inflammation (Medrikova *et al.* 2012; Estrany *et al.*2013)and these differences in haematopoietic stem cells may contribute to this sexually dimorphic inflammatory response to HFD-induced obesity and insulin resistance (Singer *et al.* 2015).

These mechanistic data corroborate several clinical and experimental studies that showed that inactivating mutations of ERα in human recapitulate aspects of the metabolic syndrome (Smith *et al.* 1994; Yoshihara *et al.* 2009), and diminished ERα expression is associated with obesity, and consequently, insulin resistance in women (Nilsson *et al.* 2007), while male and female ERα knockout mice displayed increased weight gain and fat mass associated with impaired glucose tolerance and insulin resistance (Heine *et al.* 2000), and ERα agonist-treated mice fed a HFD diet improved insulin sensitivity (Hamilton *et al.* 2016). Also corroborating our study, macrophage specific ERα knockout mice are prone to inflammation and insulin resistance (Ribas *et al.* 2011).

Inflammation has emerged as a central underpinning in obesity-induced insulin resistance as reflected by the observations of severe insulin resistance in septic patients (Clowes *et al.* 1978; Iochida *et al.* 1989) and increased plasma cytokine concentrations in insulin-resistant obese and diabetic subjects (Visser *et al.* 1999; Yudkin *et al.* 2000). Later studies in obese rodents that display insulin resistance demonstrated increased TNFα in adipose tissue (Hotamisligil *et al.* 1993) which decreased with weight reduction (Hotamisligil *et al.* 1995). Increased adipose tissue macrophages recruitment plays a predominant role in pro-inflammatory cytokine production in obesity (Xu *et al.* 2003; Weisberg *et al.* 2006). Several studies have demonstrated that pro-inflammatory cytokines, such as TNF-α, increase WAT lipolysis (Kawakami *et al.* 1987; Perry *et al.* 2015), although the underlying mechanism is unclear. Furthermore, IL-6 infusion in healthy humans increases plasma fatty acid and glycerol concentrations (indirect measures of WAT lipolysis) (Watt *et al.* 2005), and IL-6 infusion also increased WAT lipolysis in rodents and reduced insulin-stimulated suppression of lipolysis (Perry *et al.* 2015). Thus, adipose tissue inflammation may increase lipolysis, consistent with our data showing reduced insulin-stimulated suppression of WAT lipolysis in HFD fed male mice associated with increased WAT inflammation compared with female mice. This, in turn, may have contributed to insulin resistance, by which the lipolysis excess could induce an increased flux of NEFA to liver and muscle and, consequently, drive fatty

acid re-esterification and ectopic lipid accumulation, leading to the associated impairments in insulin signalling. This mechanism of increased NEFA flux to drive fatty acid re-esterification and ectopic lipid accumulation, independently of insulin action or other factors, has been demonstrated recently by our group (Vatner *et al.* 2015).

The association between ectopic lipid accumulation and insulin resistance is widely accepted. Several studies have shown this strong causal relationship between ectopic lipid accumulation and hepatic and muscle insulin resistance (Cantley *et al.* 2013; Camporez *et al.* 2015, 2017; Petersen *et al.* 2016; Samuel & Shulman, 2016; Abulizi *et al.* 2017), and our data clearly showed this association between reduced ectopic lipid content (DAG in particular) and protection against obesity-induced insulin resistance in female mice (and E2-treated male mice). This protection against obesity-induced insulin resistance was also observed in humans, with women being protected when compared with men (Frias *et al.* 2001; Hoeg *et al.* 2011), and in rats (Hevener *et al.* 2002). The major lipid intermediary is DAG, which activates members of the PKC family. Muscle lipid accumulation is associated with activation of a novel PKC (isoform PKCθ), providing a potential link between lipid accumulation and alteration in insulin sensitivity. This link between DAG-mediated activation of PKCθ and muscle insulin resistance has been replicated in human studies (Itani *et al.* 2002; Szendroedi *et al.* 2014) as well as mouse/rat studies (Galbo *et al.* 2013; Camporez *et al.* 2013b, 2017). Together, these studies support the paradigm that DAG accumulation in muscle can lead to muscle insulin resistance through activation of PKCθ. A similar mechanism has also been demonstrated in liver. The hepatic accumulation of DAG activates a novel PKC (isoform PKCε), which promotes increased phosphorylation of a critical threonine in the catalytic subunit of the IRK (threonine^{1160} human IRK, threonine^{1150} mouse IRK) leading to decreased IRK tyrosine phosphorylation and reduced IRK activity (Petersen *et al.* 2016). Taken together, these studies demonstrate that ectopic lipid accumulation within the liver can specifically cause hepatic insulin resistance.

In summary, we have shown that both female mice and E2-treated male mice are protected against obesity-induced whole-body insulin resistance, which in turn could be attributed to protection from lipid-induced insulin resistance in liver, skeletal muscle and WAT. This protection against obesity-induced insulin resistance in liver and skeletal muscle was associated with reduced ectopic lipid (DAG) content and reduced PKCε and PKCθ activation in liver and muscle, respectively. Both HFD female mice and E2-treated male mice also manifested improved insulin-stimulated suppression of WAT lipolysis, which was associated with reduced plasma and adipose tissue cytokines. Taken together, our data suggest that E2 plays an important role in mediating protection against HFD-induced WAT inflammation, which improves insulin action in suppressing WAT lipolysis, reducing the delivery of fatty acids to liver and muscle, and protecting against ectopic lipid-induced liver and muscle insulin resistance.

Acknowledgements

We thank Ali Nasiri, Gina Butrico and Mario Kahn for their invaluable technical assistance.

Funding

This work was funded by the following grants: K99AG058801 (ELG), P01AG051459, AI105097, AR070811, AG043608 (VDD), R01 DK-116774, P30 DK-45735, R01 AG-23686, an ADA-Distinguished Clinical Investigator Award (K.F.P.), a K01 DK-099402 (M.J.J.), an ADA-Merck Mentor Based Clinical/Translational Science Postdoctoral Fellowship Award (1-14-10 Merck) (G.I.S.) from the American Diabetes Association, and CAPES 88887.144251/2017-00 and CNPq 211490/2013-4 (J.P.C.).

Biography

Joao Paulo Camporez, PhD, is an Assistant Professor of Human Physiology in the Department of Physiology and Biophysics in the Institute of Biomedical Sciences at the University of Sao Paulo. He completed his graduate training at the University of Sao Paulo and was a postdoctoral fellow at Yale University School of Medicine where he joined the research faculty and served as Co-Director of the NIH-funded Yale Mouse Metabolic Phenotyping Center In Vivo Metabolism Core. His lab is primary interested in the mechanisms of lipid-induced metabolic diseases, such as non-alcoholic fatty liver disease, insulin resistance and type 2 diabetes.

References

Abulizi A, Perry RJ, Camporez JPG, Jurczak MJ, Petersen KF, Aspichueta P & Shulman GI (2017). A controlled-release mitochondrial protonophore reverses hypertriglyceridemia, nonalcoholic steatohepatitis, and diabetes in lipodystrophic mice. FASEB J 31, 2916–2924. [PubMed: 28330852]

Barros RP & Gustafsson JA (2011). Estrogen receptors and the metabolic network. Cell Metab 14, 289–299. [PubMed: 21907136]

Camell CD, Sander J, Spadaro O, Lee A, Nguyen KY, Wing A, Goldberg EL, Youm YH, Brown CW, Elsworth J, Rodeheffer MS, Schultze JL & Dixit VD (2017). Inflammasome-driven catecholamine catabolism in macrophages blunts lipolysis during ageing. Nature 550, 119–123. [PubMed: 28953873]

Camporez JP, Akamine EH, Davel AP, Franci CR, Rossoni LV & Carvalho CR (2011). Dehydroepiandrosterone protects against oxidative stress-induced endothelial dysfunction in ovariectomized rats. J Physiol 589, 2585–2596. [PubMed: 21486789]

Camporez JP, Jornayvaz FR, Lee HY, Kanda S, Guigni BA, Kahn M, Samuel VT, Carvalho CR, Petersen KF, Jurczak MJ & Shulman GI (2013a). Cellular mechanism by which estradiol protects female ovariectomized mice from high-fat diet-induced hepatic and muscle insulin resistance. Endocrinology 154, 1021–1028. [PubMed: 23364948]

Camporez JP, Jornayvaz FR, Petersen MC, Pesta D, Guigni BA, Serr J, Zhang D, Kahn M, Samuel VT, Jurczak MJ & Shulman GI (2013b). Cellular mechanisms by which FGF21 improves insulin sensitivity in male mice. Endocrinology 154, 3099–3109. [PubMed: 23766126]

Camporez JP, Kanda S, Petersen MC, Jornayvaz FR, Samuel VT, Bhanot S, Petersen KF, Jurczak MJ & Shulman GI (2015). ApoA5 knockdown improves whole-body insulin sensitivity in high-fat-fed mice by reducing ectopic lipid content. J Lipid Res 56, 526–536. [PubMed: 25548259]

Camporez JP, Wang Y, Faarkrog K, Chukijrungroat N, Petersen KF & Shulman GI (2017). Mechanism by which arylamine *N*-acetyltransferase 1 ablation causes insulin resistance in mice. Proc Natl Acad Sci U S A 114, E11285–E11292. [PubMed: 29237750]

Cantley JL, Yoshimura T, Camporez JP, Zhang D, Jornayvaz FR, Kumashiro N, Guebre-Egziabher F, Jurczak MJ, Kahn M, Guigni BA, Serr J, Hankin J, Murphy RC, Cline GW, Bhanot S, Manchem VP, Brown JM, Samuel VT & Shulman GI (2013). CGI-58 knockdown sequesters diacylglycerols in

lipid droplets/ER-preventing diacylglycerol-mediated hepatic insulin resistance. Proc Natl Acad Sci U S A 110, 1869–1874. [PubMed: 23302688]

Clowes GH Jr, Martin H, Walji S, Hirsch E, Gazitua R & Goodfellow R (1978). Blood insulin responses to blood glucose levels in high output sepsis and septic shock. Am J Surg 135, 577–583. [PubMed: 345832]

de Lima-Salgado TM, Alba-Loureiro TC, do Nascimento CS, Nunes MT & Curi R (2011). Molecular mechanisms by which saturated fatty acids modulate TNF-α expression in mouse macrophage lineage. Cell Biochem Biophys 59, 89–97. [PubMed: 20809180]

Donahue RP, Bean JA, Donahue RA, Goldberg RB & Prineas RJ (1997). Insulin response in a triethnic population: effects of sex, ethnic origin, and body fat. Miami Community Health Study. Diabetes Care 20, 1670–1676. [PubMed: 9353606]

Estrany ME, Proenza AM, Gianotti M & Llado I (2013).High-fat diet feeding induces sex-dependent changes in inflammatory and insulin sensitivity profiles of rat adipose tissue. Cell Biochem Funct 31, 504–510. [PubMed: 23112138]

Estrany ME, Proenza AM, Llado I & Gianotti M (2011). Isocaloric intake of a high-fat diet modifies adiposity and lipid handling in a sex dependent manner in rats. Lipids Health Dis 10, 52. [PubMed: 21486445]

Folch J, Lees M & Sloane Stanley GH (1957). A simple method for the isolation and purification of total lipides from animal tissues. J Biol Chem 226, 497–509. [PubMed: 13428781]

Foryst-Ludwig A, Clemenz M, Hohmann S, Hartge M, Sprang C, Frost N, Krikov M, Bhanot S, Barros R, Morani A, Gustafsson JA, Unger T & Kintscher U (2008). Metabolic actions of estrogen receptor beta (ERβ) are mediated by a negative cross-talk with PPARγ. PLoS Genet 4, e1000108. [PubMed: 18584035]

Frias JP, Macaraeg GB, Ofrecio J, Yu JG, Olefsky JM & Kruszynska YT (2001). Decreased susceptibility to fatty acid-induced peripheral tissue insulin resistance in women. Diabetes 50, 1344–1350. [PubMed: 11375335]

Galbo T, Perry RJ, Jurczak MJ, Camporez JP, Alves TC, Kahn M, Guigni BA, Serr J, Zhang D, Bhanot S, Samuel VT & Shulman GI (2013). Saturated and unsaturated fat induce hepatic insulin resistance independently of TLR-4 signaling and ceramide synthesis in vivo. Proc Natl Acad Sci U S A 110, 12780–12785. [PubMed: 23840067]

Grundy D (2015). Principles and standards for reporting animal experiments in *The Journal of Physiology* and *Experimental Physiology*. J Physiol 593, 2547–2549. [PubMed: 26095019]

Hamilton DJ, Minze LJ, Kumar T, Cao TN, Lyon CJ, Geiger PC, Hsueh WA & Gupte AA (2016). Estrogen receptor alpha activation enhances mitochondrial function and systemic metabolism in high-fat-fed ovariectomized mice. Physiol Rep 4, e12913. [PubMed: 27582063]

Heine PA, Taylor JA, Iwamoto GA, Lubahn DB & Cooke PS (2000). Increased adipose tissue in male and female estrogen receptor-α knockout mice. Proc Natl Acad Sci U S A 97, 12729–12734. [PubMed: 11070086]

Hevener A, Reichart D, Janez A & Olefsky J (2002). Female rats do not exhibit free fatty acid-induced insulin resistance. Diabetes 51, 1907–1912. [PubMed: 12031980]

Hoeg L, Roepstorff C, Thiele M, Richter EA, Wojtaszewski JF & Kiens B (2009). Higher intramuscular triacylglycerol in women does not impair insulin sensitivity and proximal insulin signaling. J Appl Physiol (1985) 107, 824–831. [PubMed: 19574502]

Hoeg LD, Sjoberg KA, Jeppesen J, Jensen TE, Frosig C, Birk JB, Bisiani B, Hiscock N, Pilegaard H, Wojtaszewski JF, Richter EA & Kiens B (2011). Lipid-induced insulin resistance affects women less than men and is not accompanied by inflammation or impaired proximal insulin signaling. Diabetes 60, 64–73. [PubMed: 20956497]

Hotamisligil GS (2006). Inflammation and metabolic disorders. Nature 444, 860–867. [PubMed: 17167474]

Hotamisligil GS, Arner P, Caro JF, Atkinson RL & Spiegelman BM (1995). Increased adipose tissue expression of tumor necrosis factor-alpha in human obesity and insulin resistance. J Clin Invest 95, 2409–2415. [PubMed: 7738205]

Hotamisligil GS, Shargill NS & Spiegelman BM (1993). Adipose expression of tumor necrosis factor-alpha: direct role in obesity-linked insulin resistance. Science 259, 87–91. [PubMed: 7678183]

Iochida LC, Tominaga M, Matsumoto M, Sekikawa A & Sasaki H (1989). Insulin resistance in septic rats – a study by the euglycemic clamp technique. Life Sci 45, 1567–1573. [PubMed: 2685486]

Itani SI, Ruderman NB, Schmieder F & Boden G (2002). Lipid-induced insulin resistance in human muscle is associated with changes in diacylglycerol, protein kinase C, and IκB-α. Diabetes 51, 2005–2011. [PubMed: 12086926]

Jones ME, Thorburn AW, Britt KL, Hewitt KN, Wreford NG, Proietto J, Oz OK, Leury BJ, Robertson KM, Yao S & Simpson ER (2000). Aromatase-deficient (ArKO) mice have a phenotype of increased adiposity. Proc Natl Acad Sci U S A 97, 12735–12740. [PubMed: 11070087]

Kawakami M, Murase T, Ogawa H, Ishibashi S, Mori N, Takaku F & Shibata S (1987). Human recombinant TNF suppresses lipoprotein lipase activity and stimulates lipolysis in 3T3-L1 cells. J Biochem 101, 331–338. [PubMed: 3495531]

Lovejoy JC, Champagne CM, de Jonge L, Xie H & Smith SR (2008). Increased visceral fat and decreased energy expenditure during the menopausal transition. Int J Obes (Lond) 32, 949–958. [PubMed: 18332882]

Macotela Y, Boucher J, Tran TT & Kahn CR (2009). Sex and depot differences in adipocyte insulin sensitivity and glucose metabolism. Diabetes 58, 803–812. [PubMed: 19136652]

Margolis KL, Bonds DE, Rodabough RJ, Tinker L, Phillips LS, Allen C, Bassford T, Burke G, Torrens J, Howard BV & Women's Health Initiative Investigators (2004). Effect of oestrogen plus progestin on the incidence of diabetes in postmenopausal women: results from the Women's Health Initiative Hormone Trial. Diabetologia 47, 1175–1187. [PubMed: 15252707]

Mauvais-Jarvis F, Clegg DJ & Hevener AL (2013). The role of estrogens in control of energy balance and glucose homeostasis. Endocr Rev 34, 309–338. [PubMed: 23460719]

Medrikova D, Jilkova ZM, Bardova K, Janovska P, Rossmeisl M & Kopecky J (2012). Sex differences during the course of diet-induced obesity in mice: adipose tissue expandability and glycemic control. Int J Obes (Lond) 36, 262–272. [PubMed: 21540832]

Morselli E, Frank AP, Santos RS, Fatima LA, Palmer BF & Clegg DJ (2016). Sex and gender: critical variables in pre-clinical and clinical medical research. Cell Metab 24, 203–209. [PubMed: 27508869]

Nilsson M, Dahlman I, Ryden M, Nordstrom EA, Gustafsson JA, Arner P & Dahlman-Wright K (2007). Oestrogen receptor alpha gene expression levels are reduced in obese compared to normal weight females. Int J Obes (Lond) 31, 900–907. [PubMed: 17224934]

Nuutila P, Knuuti MJ, Maki M, Laine H, Ruotsalainen U, Teras M, Haaparanta M, Solin O & Yki-Jarvinen H (1995). Gender and insulin sensitivity in the heart and in skeletal muscles. Studies using positron emission tomography. Diabetes 44, 31–36. [PubMed: 7813811]

Perry RJ, Camporez JP, Kursawe R, Titchenell PM, Zhang D, Perry CJ, Jurczak MJ, Abudukadier A, Han MS, Zhang XM, Ruan HB, Yang X, Caprio S, Kaech SM, Sul HS, Birnbaum MJ, Davis RJ, Cline GW, Petersen KF & Shulman GI (2015). Hepatic acetyl CoA links adipose tissue inflammation to hepatic insulin resistance and type 2 diabetes. Cell 160, 745–758. [PubMed: 25662011]

Petersen MC, Madiraju AK, Gassaway BM, Marcel M, Nasiri AR, Butrico G, Marcucci MJ, Zhang D, Abulizi A, Zhang XM, Philbrick W, Hubbard SR, Jurczak MJ, Samuel VT, Rinehart J & Shulman GI (2016). Insulin receptor Thr1160 phosphorylation mediates lipid-induced hepatic insulin resistance. J Clin Invest 126, 4361–4371. [PubMed: 27760050]

Previs SF, Cline GW & Shulman GI (1999). A critical evaluation of mass isotopomer distribution analysis of gluconeogenesis in vivo. Am J Physiol 277, E154–E160. [PubMed: 10409139]

Ribas V, Drew BG, Le JA, Soleymani T, Daraei P, Sitz D, Mohammad L, Henstridge DC, Febbraio MA, Hewitt SC, Korach KS, Bensinger SJ & Hevener AL (2011). Myeloid-specific estrogen receptor alpha deficiency impairs metabolic homeostasis and accelerates atherosclerotic lesion development. Proc Natl Acad Sci U S A 108, 16457–16462. [PubMed: 21900603]

Rogers NH, Perfield JW 2nd, Strissel KJ, Obin MS & Greenberg AS (2009). Reduced energy expenditure and increased inflammation are early events in the development of ovariectomy-induced obesity. Endocrinology 150, 2161–2168. [PubMed: 19179442]

Samuel VT & Shulman GI (2016). The pathogenesis of insulin resistance: integrating signaling pathways and substrate flux. J Clin Invest 126, 12–22. [PubMed: 26727229]

Singer K, Maley N, Mergian T, DelProposto J, Cho KW, Zamarron BF, Martinez-Santibanez G, Geletka L, Muir L, Wachowiak P, Demirjian C & Lumeng CN (2015). Differences in hematopoietic stem cells contribute to sexually dimorphic inflammatory responses to high fat diet-induced obesity. J Biol Chem 290,13250–13262. [PubMed: 25869128]

Smith EP, Boyd J, Frank GR, Takahashi H, Cohen RM, Specker B, Williams TC, Lubahn DB & Korach KS (1994). Estrogen resistance caused by a mutation in the estrogen-receptor gene in a man. N Engl J Med 331, 1056–1061. [PubMed: 8090165]

Szendroedi J, Yoshimura T, Phielix E, Koliaki C, Marcucci M,Zhang D, Jelenik T, Muller J, Herder C, Nowotny P, Shulman GI & Roden M (2014). Role of diacylglycerol activation of PKCθ in lipid-induced muscle insulin resistance in humans. Proc Natl Acad Sci U S A 111, 9597–9602. [PubMed: 24979806]

Vatner DF, Majumdar SK, Kumashiro N, Petersen MC, Rahimi Y, Gattu AK, Bears M, Camporez JP, Cline GW, Jurczak MJ, Samuel VT & Shulman GI (2015). Insulin-independent regulation of hepatic triglyceride synthesis by fatty acids. Proc Natl Acad Sci U S A 112, 1143–1148. [PubMed: 25564660]

Visser M, Bouter LM, McQuillan GM, Wener MH & Harris TB (1999). Elevated C-reactive protein levels in overweight and obese adults. JAMA 282, 2131–2135. [PubMed: 10591334]

Watt MJ, Carey AL, Wolsk-Petersen E, Kraemer FB, Pedersen BK & Febbraio MA (2005). Hormone-sensitive lipase is reduced in the adipose tissue of patients with type 2 diabetes mellitus: influence of IL-6 infusion. Diabetologia 48, 105–112. [PubMed: 15609025]

Weisberg SP, Hunter D, Huber R, Lemieux J, Slaymaker S,Vaddi K, Charo I, Leibel RL & Ferrante AW Jr (2006). CCR2 modulates inflammatory and metabolic effects of high-fat feeding. J Clin Invest 116, 115–124. [PubMed: 16341265]

Wu X, Tong Y, Shankar K, Baumgardner JN, Kang J, Badeaux J,Badger TM & Ronis MJ (2011). Lipid fatty acid profile analyses in liver and serum in rats with nonalcoholic steatohepatitis using improved gas chromatography-mass spectrometry methodology. J Ag Food Chem 59, 747–754.

Xu H, Barnes GT, Yang Q, Tan G, Yang D, Chou CJ, Sole J,Nichols A, Ross JS, Tartaglia LA & Chen H (2003). Chronic inflammation in fat plays a crucial role in the development of obesity-related insulin resistance. J Clin Invest 112, 1821–1830. [PubMed: 14679177]

Yoshihara R, Utsunomiya K, Gojo A, Ishizawa S, Kanazawa Y, Matoba K, Taniguchi K, Yokota T, Kurata H, Yokoyama J, Urashima M & Tajima N (2009). Association of polymorphism of estrogen receptor-α gene with circulating levels of adiponectin in postmenopausal women with type 2 diabetes. J Atheroscler Thromb 16, 250–255. [PubMed: 19556726]

Yudkin JS, Kumari M, Humphries SE & Mohamed-Ali V (2000). Inflammation, obesity, stress and coronary heart disease: is interleukin-6 the link? Atherosclerosis 148, 209–214. [PubMed: 10657556]

Key points

- Oestrogen has been shown to play an important role in the regulation of metabolic homeostasis and insulin sensitivity in both human and rodent studies.
- Insulin sensitivity is greater in premenopausal women compared with age-matched men, and metabolism-related cardiovascular diseases and type 2 diabetes are less frequent in these same women.
- Both female and male mice treated with oestradiol are protected against obesity-induced insulin resistance.
- The protection against obesity-induced insulin resistance is associated with reduced ectopic lipid content in liver and skeletal muscle.
- These results were associated with increased insulin-stimulated suppression of white adipose tissue lipolysis and reduced inflammation.

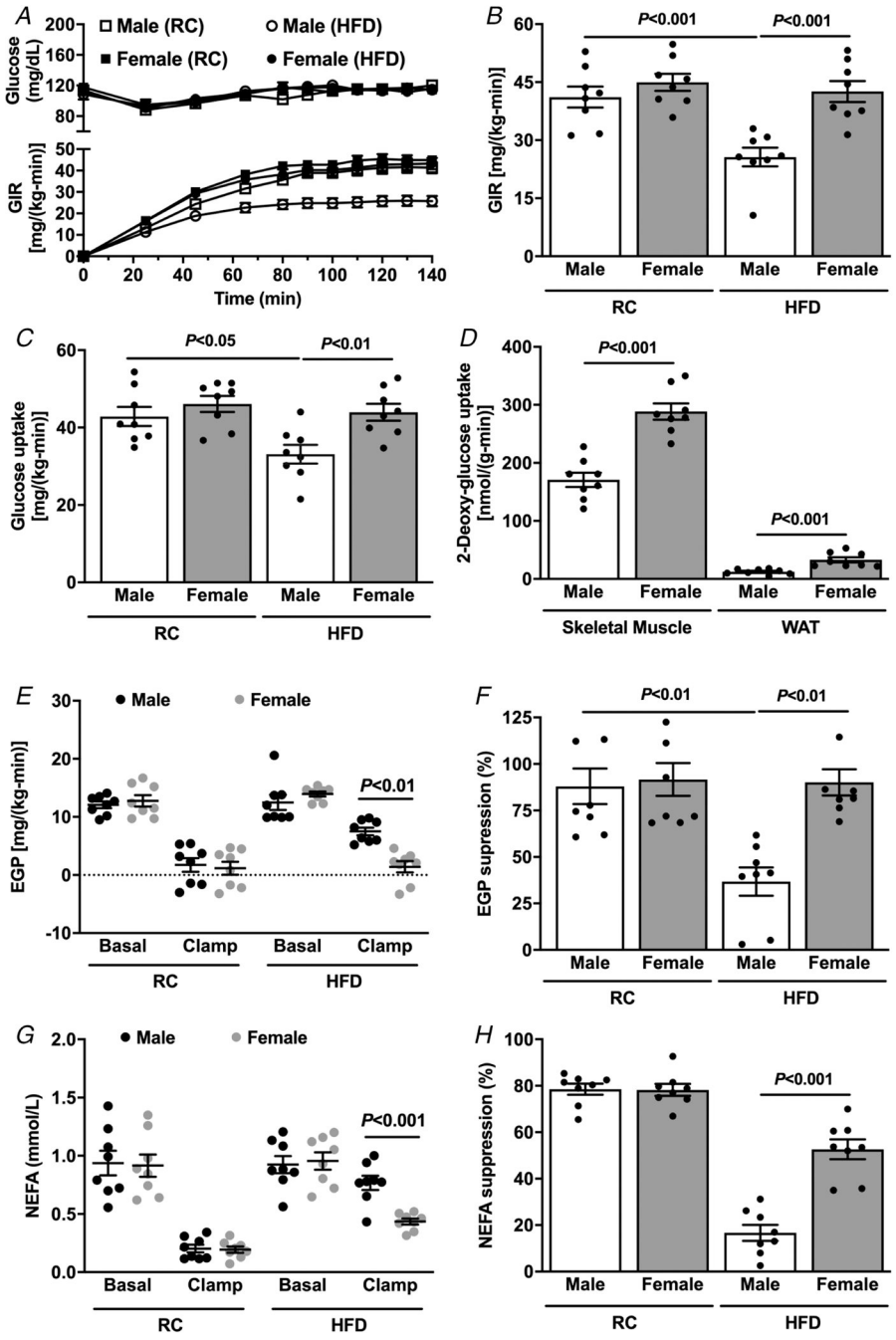

Figure 1. Age-matched female mice are protected against HFD-induced insulin resistance

A, plasma glucose and glucose infusion rate (GIR) during the course of the hyperinsulinaemic–euglycaemic clamp. *B*, average of GIR during the steady-state (last 40 min) of the hyperinsulinaemic–euglycaemic clamp. *C*, whole-body glucose uptake (R_d) during the hyperinsulinaemic–euglycaemic clamp. *D*, tissue specific 2-deoxyglucose uptake during the hyperinsulinaemic–euglycaemic clamp. *E* and *F*, endogenous glucose production and suppression (%) during basal and hyperinsulinaemic–euglycaemic clamp. *G* and *H*, non-

esterified fatty acids (NEFA) and suppression (%) during basal and hyperinsulinaemic–euglycaemic clamp. Data are means ± SEM.

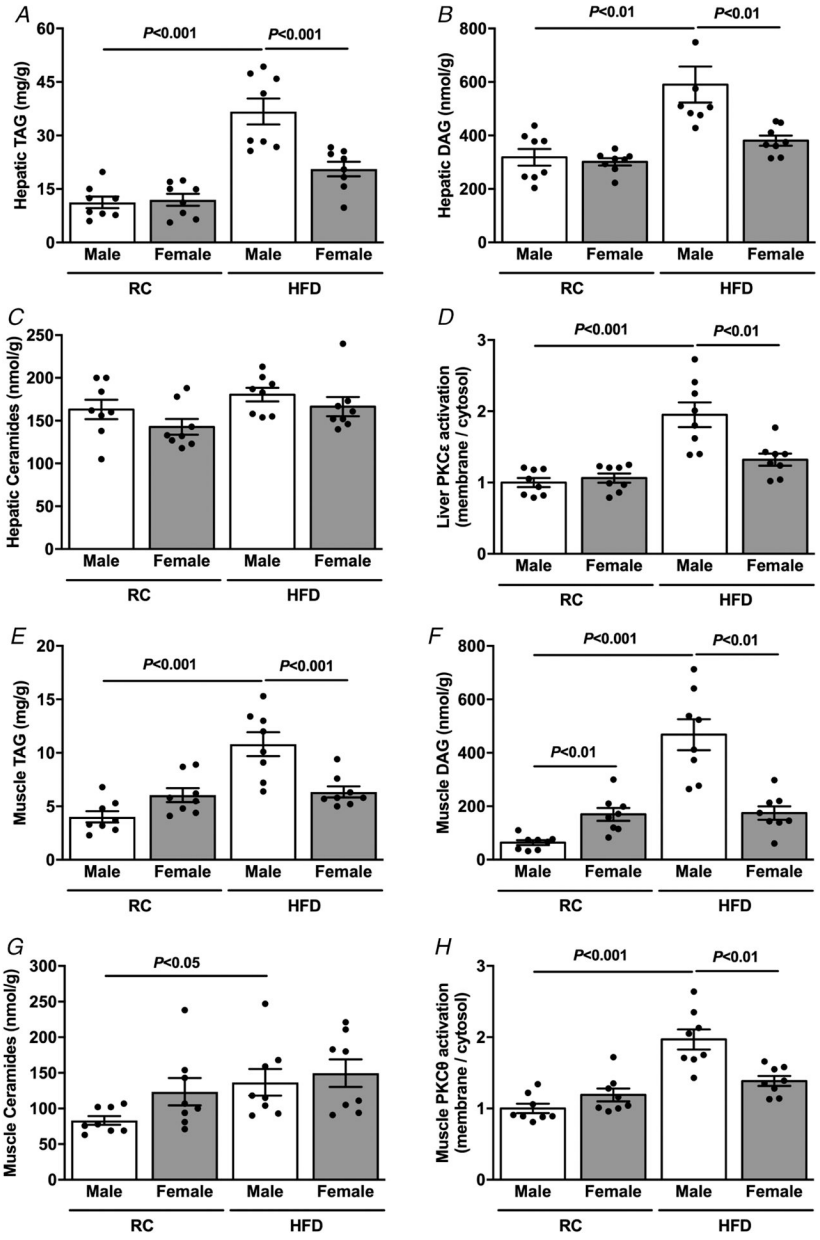

Figure 2. Age-matched female mice are protected against HFD-induced ectopic lipid accumulation

A, basal hepatic TAG content. *B*, basal hepatic DAG content. *C*, basal hepatic ceramide content. *D*, basal liver PKCε activation. *E*, basal muscle TAG content. *F*, basal muscle membrane DAG content. *G*, basal muscle ceramide content. *H*, basal muscle PKCθ activation. Data are means ± SEM.

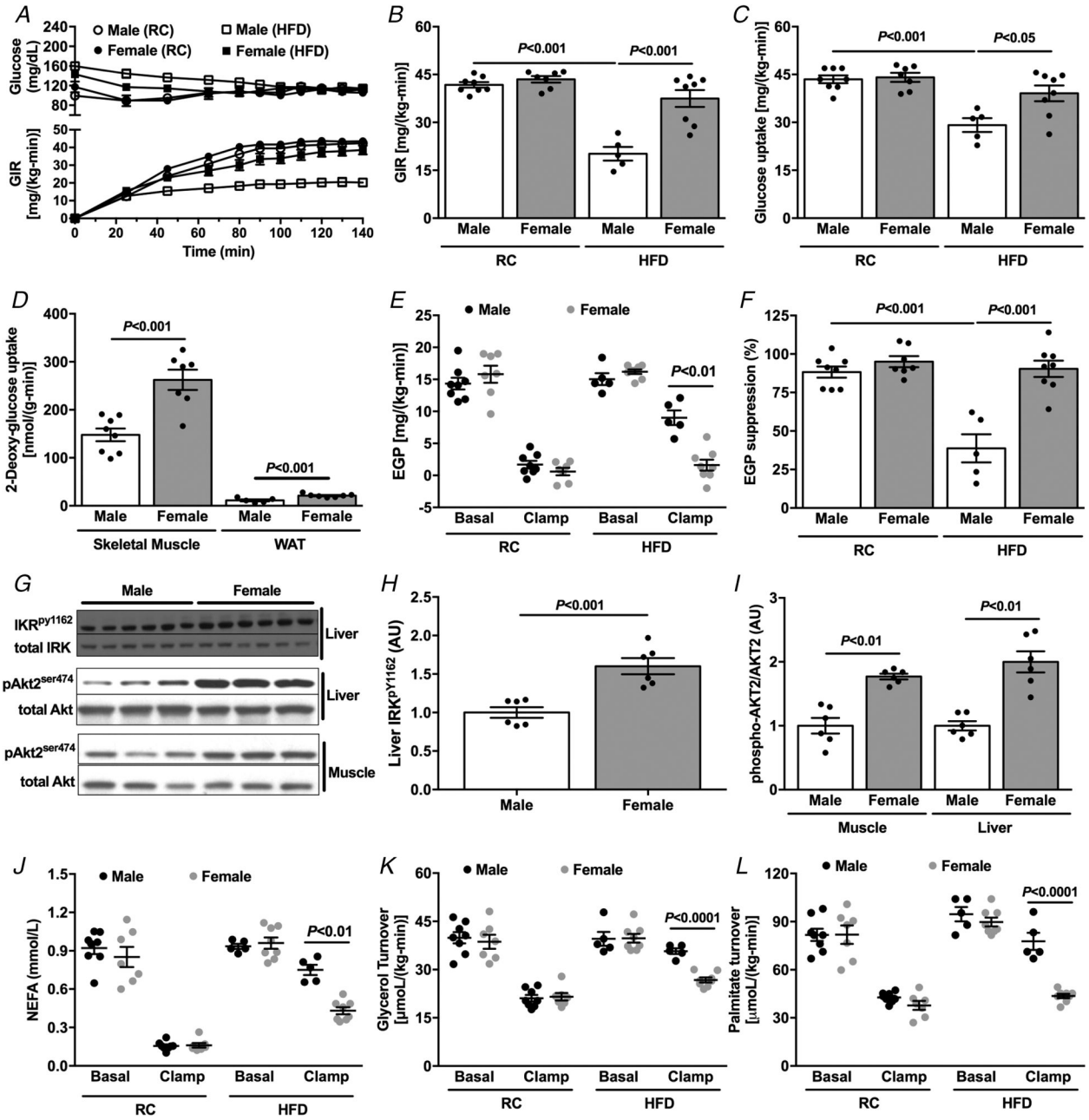

Figure 3. Body weight-matched female mice are protected against HFD-induced insulin resistance

A, plasma glucose and glucose infusion rate (GIR) during the course of the hyperinsulinaemic–euglycaemic clamp. *B*, average of GIR during the steady-state (last 40 min) of the hyperinsulinaemic–euglycaemic clamp. *C*, whole-body glucose uptake (R_d) during the hyperinsulinaemic–euglycaemic clamp. *D*, tissue specific 2-deoxyglucose uptake during the hyperinsulinaemic–euglycaemic clamp. *E* and *F*, endogenous glucose production and suppression (%) during basal and hyperinsulinaemic–euglycaemic clamp. *G–I*, western blot images and quantification for insulin-stimulated IRK tyrosine^{1162} phosphorylation and Akt2 phosphorylation in HFD-fed male and female mice. *J*, non-esterified fatty acids

(NEFA) during basal and hyperinsulinaemic–euglycaemic clamp. *K* and *L*, glycerol and palmitate turnover during basal and hyperinsulinaemic–euglycaemic clamp. Data are means ± SEM.

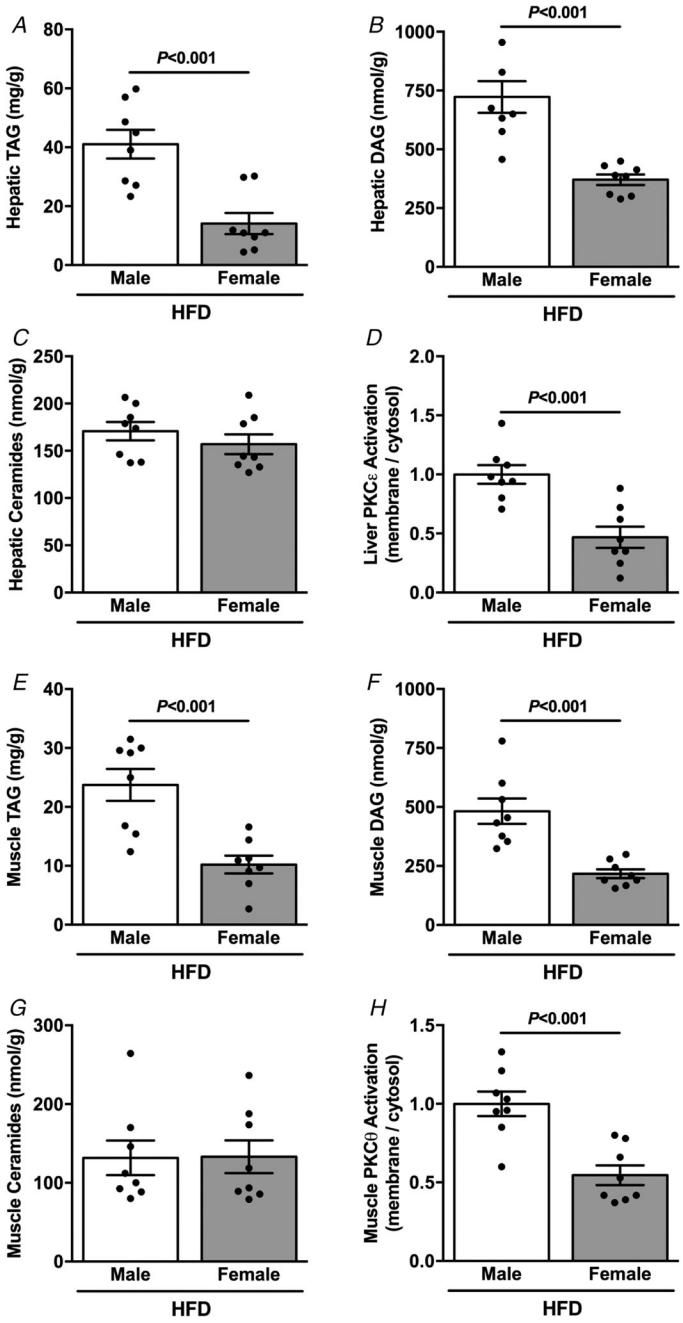

Figure 4. Body weight-matched female mice are protected against HFD-induced ectopic lipid accumulation

A, basal hepatic TAG content. *B*, basal hepatic DAG content. *C*, basal hepatic ceramide content. *D*, basal liver PKCε activation. *E*, basal muscle TAG content. *F*, basal muscle membrane DAG content. *G*, basal muscle ceramide content. *H*, basal muscle PKCθ activation. Data are means ± SEM.

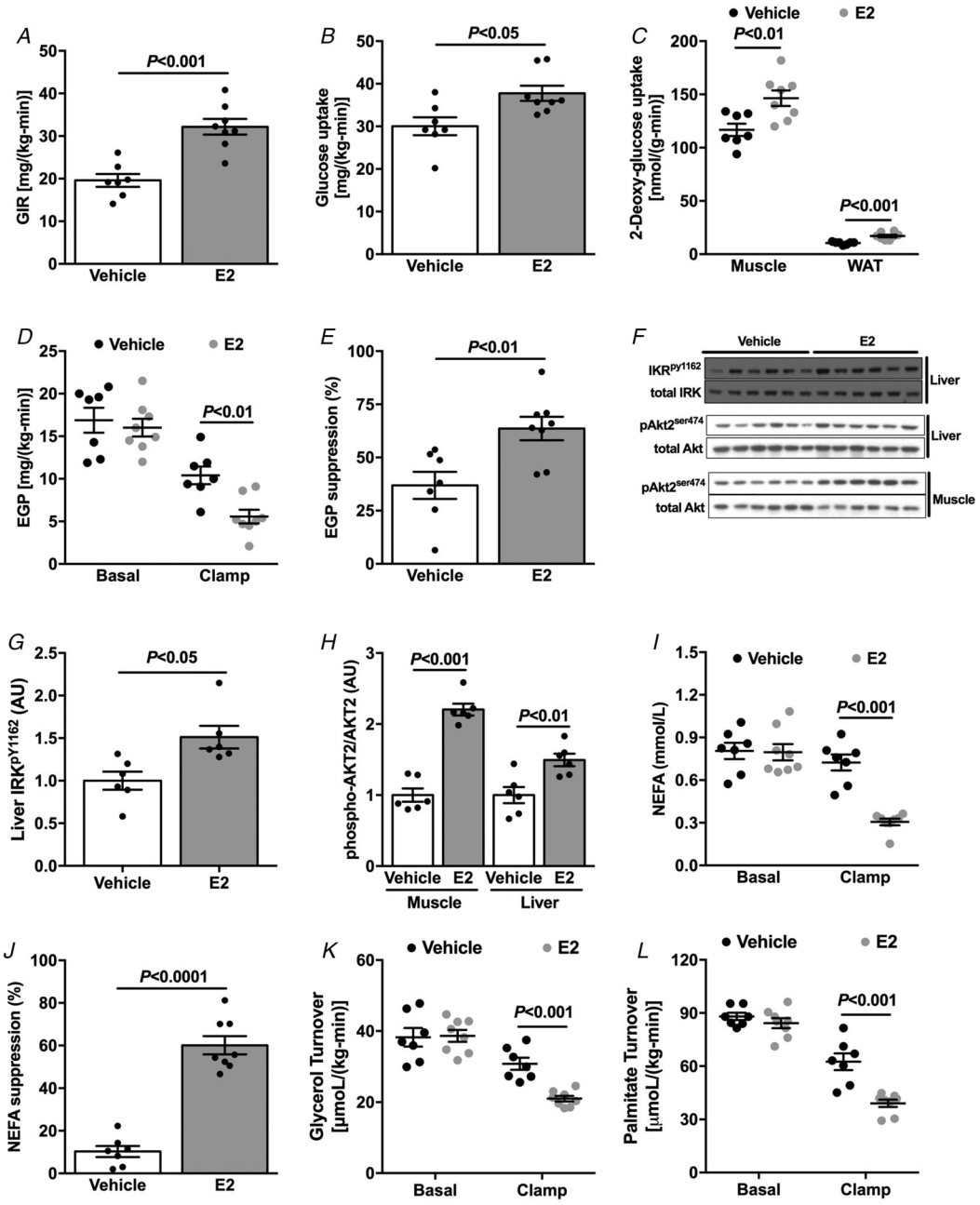

Figure 5. Oestradiol-treated male mice are protected against HFD-induced insulin resistance

A, average of GIR during the steady-state (last 40 min) of the hyperinsulinaemic–euglycaemic clamp. *B*, whole-body glucose uptake (R_d) during the hyperinsulinaemic–euglycaemic clamp. *C*, tissue specific 2-deoxyglucose uptake during the hyperinsulinaemic–euglycaemic clamp. *D* and *E*, endogenous glucose production and suppression (%) during basal and hyperinsulinaemic–euglycaemic clamp. *F–H*, western blot images and quantification for insulin-stimulated IRK tyrosine^{1162} phosphorylation and Akt2 phosphorylation. *I* and *J*, non-esterified fatty acids (NEFA) and suppression (%) during basal and hyperinsulinaemic–euglycaemic clamp. *K* and *L*, glycerol and palmitate turnover during basal and hyperinsulinaemic–euglycaemic clamp. Data are means ± SEM.

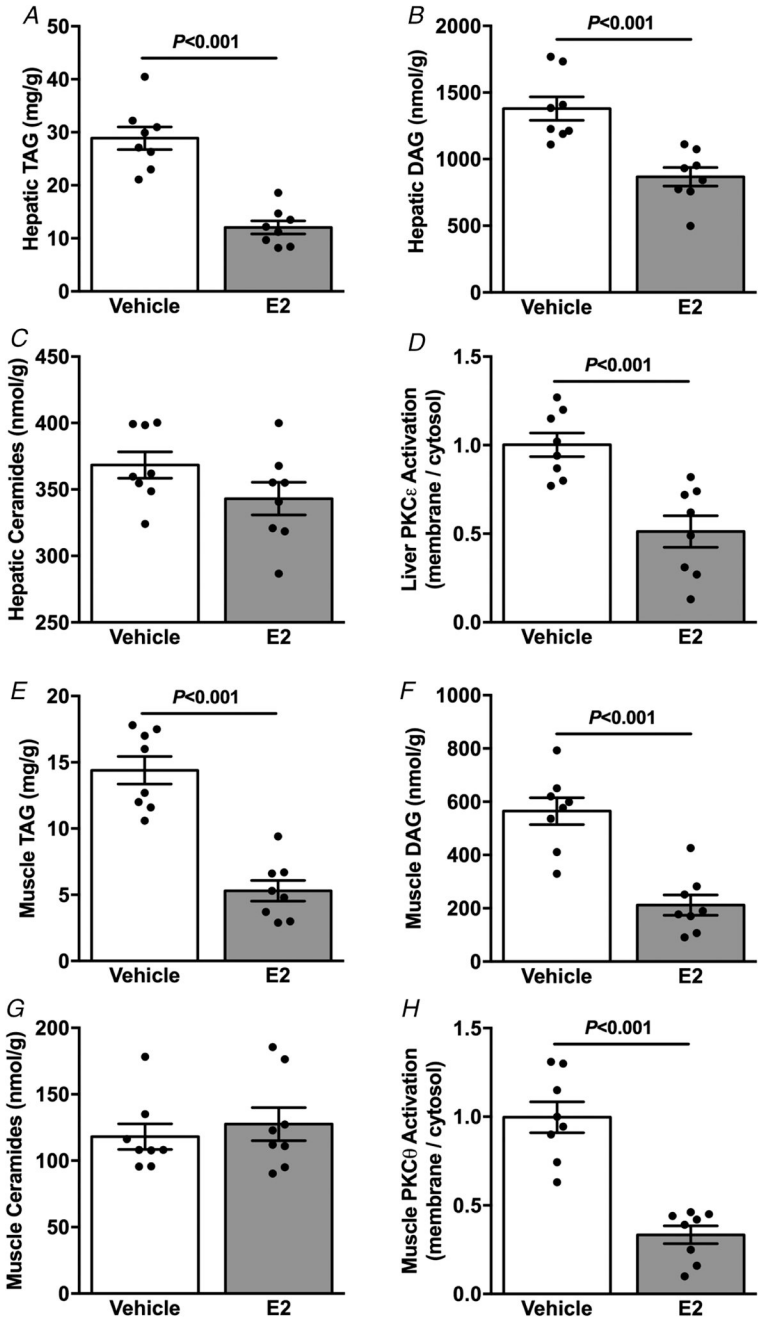

Figure 6. Oestradiol-treated male mice are protected against HFD-induced ectopic lipid accumulation

A, basal hepatic TAG content. *B*, basal hepatic DAG content. *C*, basal hepatic ceramides content. *D*, basal liver PKCε activation. *E*, basal muscle TAG content. *F*, basal muscle membrane DAG content. *G*, basal muscle ceramide content. *H*, basal muscle PKCθ activation. Data are means ± SEM.

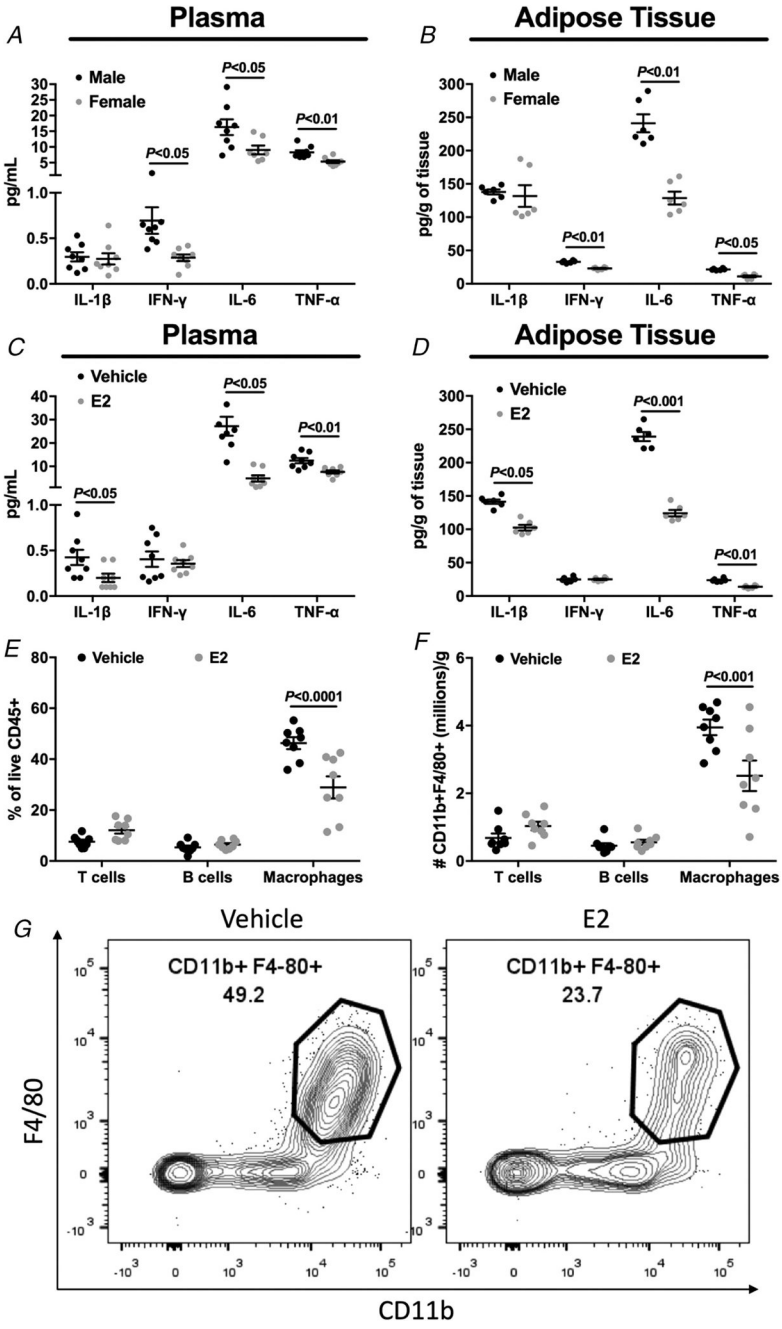

Figure 7. Body weight-matched female mice and oestradiol-treated male mice displayed reduced plasma and adipose tissue inflammation after high fat feeding

A, plasma IL-1β, IL-6, IFN-γ and TNF-α concentration in male *vs.* female mice. *B*, adipose tissue IL-1β, IL-6, IFN-γ and TNF-α concentration in male *vs.* female mice. *C*, plasma IL-1β, IL-6, IFN-γ and TNF-α concentration in vehicle *vs.* oestradiol-treated male mice. *D*, adipose tissue IL-1β, IL-6, IFN-γ and TNF-α concentration in vehicle *vs.* oestradiol-treated male mice. *E* and *F*, visceral fat immune profile from vehicle *vs.* oestradiol-treated male mice. *G*, representative flow cytometry contour plots of adipose tissue macrophages from vehicle *vs.* oestradiol-treated male mice. Data are means ± SEM.

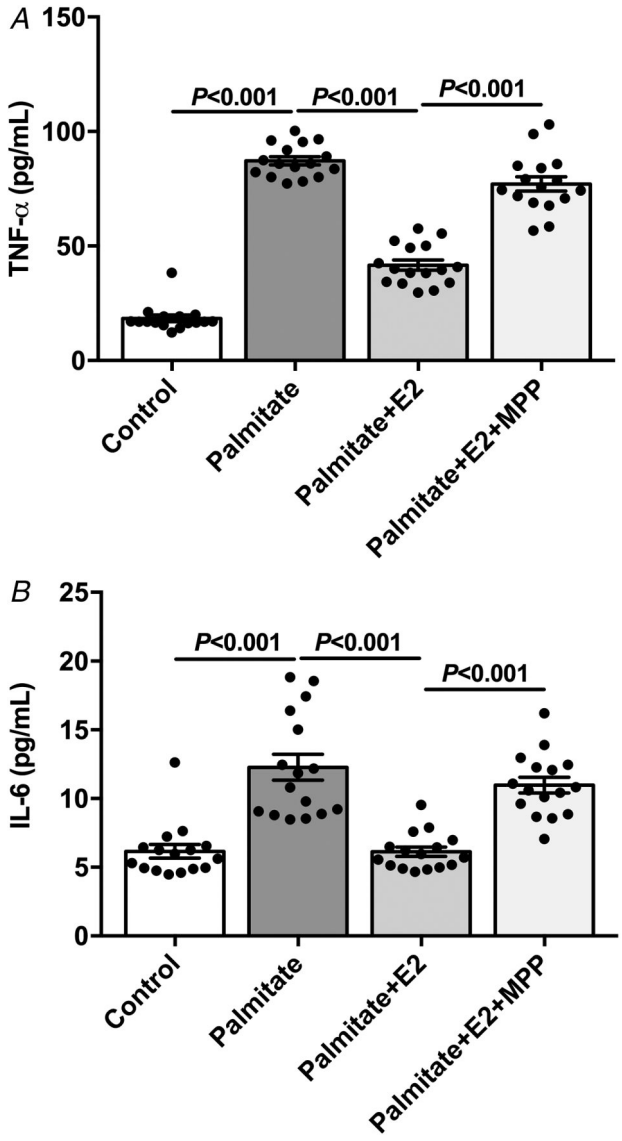

Figure 8. Oestradiol protected *in vitro* against palmitate-induced macrophage cytokine release

A, supernatant TNF-*α* concentration from macrophage cell line (J774A) culture. *B*, supernatant IL-6 concentration from macrophage cell line (J774A) culture. Data are means ± SEM.

Table 1.

Basal characterization of male and female mice at the same age (20 weeks old)

	RC		HFD	
Characteristic	**Male**	**Female**	**Male**	**Female**
Body weight (g)	28.9 ± 0.5	22.1 ± 0.4**	36.5 ± 1.6	26.6 ± 0.8**
Body fat (%)	6.9 ± 1.1	11.5 ± 0.8*	24.8 ± 2.5	21.7 ± 1.9
Fasting insulin (μU ml^{-1})	9.1 ± 3.0	6.2 ± 1	19.3 ± 1.8	9.8 ± 1.9*
Clamped insulin (μU ml^{-1})	44.6 ± 2.7	42.7 ± 3.8	52.9 ± 7.8	47.4 ± 3.7
Glucose (mg dl^{-1})	113.8 ± 3.0	117.8 ± 6	115.4 ± 1.8	111.3 ± 3.4
Energy expenditure (kcal kg^{-1} h^{-1})	16.5 ± 0.5	17.4 ± 0.3	NA	NA
RER $\left(\dot{V}_{O_2}/\dot{V}_{CO_2}\right)$	0.89 ± 0.01	0.89 ± 0.01	NA	NA
Caloric intake (kcal kg^{-1} h^{-1})	19.3 ± 1.2	16.7 ± 0.8	NA	NA
Volume drunk (ml kg^{-1} h^{-1})	1.4 ± 0.1	1.2 ± 0.1	NA	NA
Activity (counts h^{-1})	134 ± 18	210 ± 17*	NA	NA

Data are mean ± SEM of n = 8–10 mice per group.

*$P < 0.05$,

**$P < 0.01$ compared with male mice.

NA, not available.

Table 2.

Basal characterization of male (8 weeks old) and female (20 weeks old) mice with body weight-matched

	RC		HFD	
Characteristic	**Male**	**Female**	**Male**	**Female**
Body weight (g)	20.7 ± 0.5	21.0 ± 0.3	28.4 ± 0.7	27.2 ± 0.4
Body fat (%)	5.7 ± 0.2	10.6 ± 1.1 *	18.9 ± 1.8	19.4 ± 1.0
Fasting insulin (μU ml^{-1})	7.3 ± 2.5	5.8 ± 1.3	17.6 ± 2.2	9.2 ± 1.5 *
Clamped insulin (μU ml^{-1})	45.9 ± 9.0	42.9 ± 2.7	47.0 ± 4.1	45.5 ± 3.7
Glucose (mg dl^{-1})	116 ± 5.6	117 ± 11.2	160 ± 7.3	143 ± 6.8
Energy expenditure (kcal kg^{-1} h^{-1})	16.3 ± 0.6	17.3 ± 0.3	NA	NA
RER $\left(\dot{V}_{O_2}/\dot{V}_{CO_2}\right)$	0.90 ± 0.01	0.90 ± 0.01	NA	NA
Caloric intake (kcal kg^{-1} h^{-1})	21.3 ± 0.8	22.0 ± 1.4	NA	NA
Volume drunk (ml kg^{-1} h^{-1})	1.5 ± 0.2	1.7 ± 0.1	NA	NA
Activity (counts h^{-1})	265 ± 37	293 ± 27	NA	NA

Data are means ± SEM of n = 8–10 mice per group.

* $P < 0.05$ compared with male mice.

NA, not available.

Table 3.

Basal characterization of vehicle and E2-treated male mice

Characteristic	Vehicle	E2
Body weight (g)	31.6 ± 1.2	30.6 ± 0.6
Body fat (%)	17.6 ± 2.3	8.1 ± 1.4**
Lean mass (g)	20.5 ± 0.5	22.3 ± 0.6*
Plasma testosterone (ng ml^{-1})	1.25 ± 0.3	1.0 ± 0.3
Fasting insulin (μU ml^{-1})	14.8 ± 3.0	6.9 ± 1.7*
Clamped insulin (μU ml^{-1})	46.4 ± 9.4	42.1 ± 4.4
Glucose (mg dl^{-1})	166.1 ± 14.6	150.4 ± 7.8
Energy expenditure (kcal kg^{-1} h^{-1})	14.8 ± 0.6	17.0 ± 0.5*
RER $\left(\dot{V}_{O_2}/\dot{V}_{CO_2}\right)$	0.78 ± 0.005	0.79 ± 0.005
Caloric intake (kcal kg^{-1} h^{-1})	16.2 ± 1.4	20.3 ± 1.1*
Volume drunk (ml kg^{-1} h^{-1})	1.0 ± 0.1	1.5 ± 0.1*
Activity (counts h^{-1})	205 ± 23	173 ± 34

Data are means ± SEM of n = 8–10 mice per group.

* $P < 0.05$,

** $P < 0.01$ compared with vehicle-treated mice.